



## Macromolecular Nanotechnology

# The change in the environment of the immiscible block stabilizes an unexpected HPC phase in a cured block copolymer/epoxy blend



Agustina B. Leonardi, Ileana A. Zucchi, Roberto J.J. Williams\*

Institute of Materials Science and Technology (INTEMA), University of Mar del Plata and National Research Council (CONICET), Av. J. B. Justo 4302, 7600 Mar del Plata, Argentina

## ARTICLE INFO

## Article history:

Received 5 June 2015

Received in revised form 15 July 2015

Accepted 29 July 2015

Available online 30 July 2015

## Keywords:

Block copolymer

Block copolymer/epoxy blends

Lamellar to hexagonal transformation

Polymerization-induced self-assembly

PS-*b*-PEO/epoxy

SAXS spectra

## ABSTRACT

A conventional SAXS study of ordered phases produced in cured block copolymer (BCP)/epoxy blends with different concentrations, led to the unexpected observation of an HPC (hexagonally-packed cylinders) phase for a blend containing a 55:45 volume ratio of both domains. The BCP was polystyrene (PS,  $M_n = 28$  kDa)-*b*-poly(ethylene oxide) (PEO,  $M_n = 11$  kDa), where PS is the “epoxy-phobic” block and PEO is the “epoxy-philic” block. The epoxy formulation was based on diglycidylether of bisphenol A (DGEBA) and 4,4'-m ethylenebis(2,6-diethylaniline) (MDEA). A fully cured blend containing 60 wt% BCP, equivalent to 45% volume fraction of PS in the blend, exhibited an unexpected HPC morphology as supported by TEM images and SAXS spectra. The same techniques showed that a lamellar (L) phase was generated at low conversions in the same blend. The L to HPC transition was explained by the diffusion of epoxy-amine species out of the PS-rich phase with the increase in conversion. Order-order transitions in BCP/epoxy blends previously reported were explained by the partial phase separation of the *miscible* block from the epoxy solvent. These transitions go always in the sense of decreasing the interface curvature (e.g., from HPC to L). The transition reported in this study goes in the opposite sense (from L to HPC) and was generated by the change in environment of the *immiscible* block during polymerization.

© 2015 Elsevier Ltd. All rights reserved.

## 1. Introduction

Block copolymer (BCP)/epoxy blends have been the subject of a large number of recent studies where the focus was placed on the role of the BCP as a processing aid [1,2], as a template for the self-assembly of different type of nanoparticles [3–5], or as a toughening agent [6–19]. The nanostructuring of the BCP in the epoxy matrix requires an immiscible block, either initially [20,21] or during polymerization [22,23], and another block that keeps its miscibility up to high or full conversions. The latter is a necessary condition to avoid macrophase separation.

The morphology initially generated does not remain frozen but can evolve with conversion. Order-order transitions can take place by the fact that the reactive solvent becomes less compatible with the miscible block as conversion increases. Chains of the miscible block can evolve from “wet” brushes swollen by the reactive solvent to partially collapsed “dry”

\* Corresponding author.

E-mail address: [williams@fi.mdp.edu.ar](mailto:williams@fi.mdp.edu.ar) (R.J.J. Williams).

brushes. This can produce order-order transitions that decrease the interfacial curvature. Lipic et al. [21] analyzed the self-assembly of poly(ethylene oxide)-*b*-poly(ethylene-*alt*-propylene) (PEO-*b*-PEP), in an epoxy formulation, where PEO was the “epoxy-philic” block and PEP the “epoxy-phobic” one. For one particular formulation, they reported the transformation of a gyroid (G) to a lamellar (L) phase, just prior to gelation; for another formulation they observed a transition from a cubic packed spherical morphology to a hexagonal phase. These transformations were explained by the decrease of the miscibility of PEO with the epoxy polymer by increasing conversion (the “wet” to “dry” brush concept). In turn, Romeo et al. [24] analyzed the self-assembly of a polystyrene-*b*-poly(methyl methacrylate) (PS-*b*-PMMA), in an epoxy formulation, where PMMA was the “epoxy-philic” block and PS the “epoxy-phobic” one. Spherical micelles generated at low conversions were transformed to a cubic packed spherical morphology (S), then to columns of spherical micelles, ending in a hexagonally packed cylinders (HPC) phase. Again, these transitions were explained by the decrease in the solubility of the PMMA block with conversion. It was also shown that by a particular selection of the cure cycle these transformations could be reverted. By increasing temperature at an intermediate conversion, the solubility of PMMA in the epoxy was increased (PMMA exhibits an upper-critical-solution-temperature in epoxy formulations). This produced a reversion of the HPC phase to columns of spherical micelles (“dry” brushes became “wet” again by the temperature increase). This morphology was frozen at complete conversion.

However, no attention has been paid to the consequences of the partition of the reactive solvent between both phases. When phase separation (nanostructuration) takes place, thermodynamics predicts that a fraction of the reactive solvent enriched in monomers and short oligomers must segregate together with the immiscible block [25–29]. As polymerization continues in the phase rich in the immiscible block, the largest oligomers are no longer miscible and diffuse out of this phase. This has two different consequences. The obvious one is the continuous variation of the volume ratio between both phases that might convey the system to cross the stability limit between different ordered phases. This is analogous to the order-order transitions observed in solutions of a BCP when adding increasing amounts of a highly selective solvent for one of the blocks [30]. The second less obvious consequence derives from the fact that the reactive solvent species segregated with the immiscible block behave as a poor solvent that turns into a no-solvent as polymerization continues in this phase. Conformation of coils of the immiscible block must gradually change from an initial collapsed state to a more extended theta state as the reactive solvent species diffuse out of this phase. This might produce an unexpected order-order transition, generating an ordered phase outside the stability limits corresponding to its volume fraction in the blend. In this study, we report experimental evidence of such a transition for a particular BCP/epoxy blend.

## 2. Experimental section

### 2.1. Materials

The epoxy monomer was based on diglycidylether of bisphenol A (DGEBA), with an epoxy equivalent of 179 g/mol, determined by chemical titration. The hardener was 4,4'-methylenebis(2,6-diethylaniline) (MDEA, Aldrich), used in an almost stoichiometric proportion (stoichiometric epoxy/amine ratio equal to 0.974 in equivalents of both monomers). The BCP was a commercial polystyrene (PS)-*b*-poly(ethylene oxide) (PEO) (Polymer Source), with  $M_n$  (PS) = 28 kDa and  $M_n$  (PEO) = 11 kDa, and a polydispersity index,  $PI$  = 1.11.

### 2.2. Synthesis and cure of blends

First, DGEBA was blended with the BCP, in proportions giving 40–60 wt% BCP in the final cured material. The dissolution was performed in a silicon mold adding a small amount of toluene to facilitate the process. Toluene was then removed at 60 °C during several hours until a constant weight was obtained. Then, temperature was increased to 80 °C and MDEA added with continuous stirring. The polymerization was carried out at 135 °C during 4 h. The nanostructures generated were analyzed at this stage (partial conversion) and after a thermal treatment at 190 °C for another 4 h under nitrogen (full conversion).

### 2.3. Characterization techniques

Near-infrared spectroscopy was used to follow the conversion of epoxy groups during polymerization at 135 °C, determined by measuring the height of the absorption band of epoxy groups at about 4525  $\text{cm}^{-1}$  with respect to the height of a reference band at about 4615  $\text{cm}^{-1}$ . A Nicolet 6700 FTIR device, equipped with a heated transmission cell (HT-32, Spectra Tech) with glass windows (32 mm diameter, 1.4 mm rubber spacer), and a programmable temperature controller (Omega, Spectra Tech, DTZG1 8C), was employed.

Transmission Electron Microscopy (TEM) images were recorded at room temperature using a JEOL 100CX device. Thin sections were obtained employing an LKB ultramicrotome. PS blocks appeared black in the images and therefore no staining procedure was necessary.

Small-Angle X-ray Scattering (SAXS) spectra were obtained at the beamline SAXS 1 of the National Laboratory of Synchrotron Light (LNLS, Campinas, Brazil). The scattering intensity (in arbitrary units) was recorded as a function of the scattering vector  $q = (4\pi/\lambda)\sin\theta$ , where  $\lambda$  is the radiation wavelength (1.55 Å) and  $2\theta$  the scattering angle.

### 3. Results and discussion

Fig. 1 shows the evolution of the conversion of epoxy groups at 135 °C for blends containing 0, 40 and 60 wt% BCP.

The conversions attained after 4 h of cure were close to 0.90 for the neat sample, 0.78 for the blend with 40 wt% BCP and 0.12 for the blend with 60 wt% BCP. The presence of the BCP produced a significant decrease of the polymerization rate, particularly for the sample containing the largest BCP amount. In blends with BCP, the PS “epoxy-phobic” block is phase separated at low conversions while the PEO “epoxy-philic” block remains miscible up to very high conversions [31]. The significant decrease of the reaction rate by the BCP addition can be explained by the dilution effect produced by the large proportion of miscible PEO blocks as well as by a partial segregation of monomers and short oligomers to the PS-rich phase.

FTIR spectra of the neat sample and of blends containing 40–60 wt% BCP, partially cured during 4 h at 135 °C and post-cured another 4 h at 190 °C, showed complete disappearance of the characteristic epoxy peak. Under these conditions, all samples attained full conversion.

The volume fraction of PS ( $f_{PS}$ ) in the blends, may be estimated using mass fractions and densities of every component ( $PS = 1.05 \text{ g/cm}^3$ , amorphous PEO =  $1.124 \text{ g/cm}^3$  and epoxy-amine =  $1.12 \text{ g/cm}^3$ ). This leads to  $f_{PS} = 0.30$  (for 40 wt% BCP), 0.37 (for 50 wt% BCP), 0.45 (for 60 wt% BCP) and 0.73 for the neat BCP. For the fully cured BCP/epoxy blends, we assume that PEO is present in a blend with the epoxy-amine network and the other phase is neat PS. Therefore, volume fractions of PS blocks are those estimated above.

A phase diagram of PS-*b*-PEO block copolymers has been presented and discussed in the literature [32]. For  $f_{PS} = 0.73$ , an HPC (hexagonally-packed cylinders) structure composed of PEO cylinders (minority phase) in a PS matrix (majority phase), is expected. At temperatures below about 50 °C, PEO domains become crystalline. Employing differential scanning calorimetry (DSC) we verified that the neat BCP showed the melting peak of PEO at 51.5 °C and the glass transition temperature of PS at about 90 °C (results not shown).

Adding the reactive (epoxy-amine) solvent in amounts comprised between 40 and 60 wt%, had two main effects. In the first place, PEO crystallization was not observed in any of the samples, as expected [32] and as verified by DSC scans (results not shown). The second effect was that the PEO/solvent phase became the majority phase, at least in the fully cured materials. Therefore, an inverted HPC structure (PS cores in a PEO/epoxy matrix) was expected for the blend with 40 wt% BCP, because  $f_{PS} = 0.30$  is slightly less than the stability limit of this phase that, for an AB diblock copolymer, is located at about  $f_{PS} = 0.32$  [33,34]. For BCP contents equal to 50 wt% ( $f_{PS} = 0.37$ ) and 60 wt% ( $f_{PS} = 0.45$ ), a lamellar (L) morphology was expected in the fully cured blends.

Fig. 2 shows SAXS spectra of blends containing 40, 50 and 60 wt% BCP, after complete conversion at 190 °C. The progression of SAXS peaks,  $q/q_0 = 1:\sqrt{3}:\sqrt{4}:\sqrt{7}:\sqrt{9}:\sqrt{12}:\sqrt{13}:\sqrt{16}$ , corresponds to the presence of an HPC phase for the three blends, an unexpected result for the two blends with the highest BCP concentrations. For some compositions, specific peaks are not present in the progression due to the overlapping with minima of the form factor. This is the case of the peak at  $\sqrt{4}$  for the blend with 40% BCP. The suppression of this peak is expected for  $f_{cores} = f_{PS} = 0.274$  [35–37], a value that is close to the estimated volume fraction ( $f_{PS} = 0.30$ ).

The intercylinder distance can be calculated as  $d_{CYL} = 4\pi/(\sqrt{3}q_0)$  while the distance among rows of cylinders is given by  $d_{HEX} = 2\pi/q_0$  [36,38]. The following values were obtained for blends containing, respectively, 40, 50 and 60 wt% BCP:

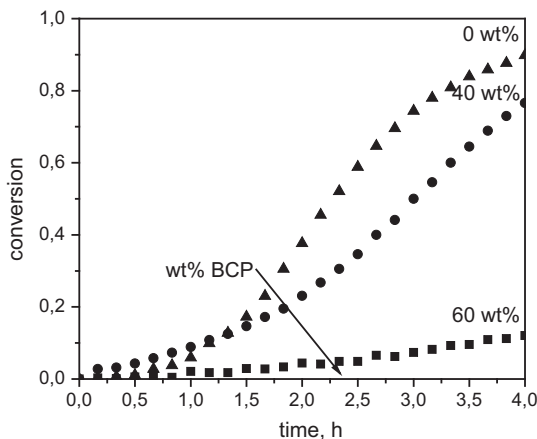


Fig. 1. Conversion of epoxy groups at 135 °C for blends containing 0, 40 and 60 wt% BCP.

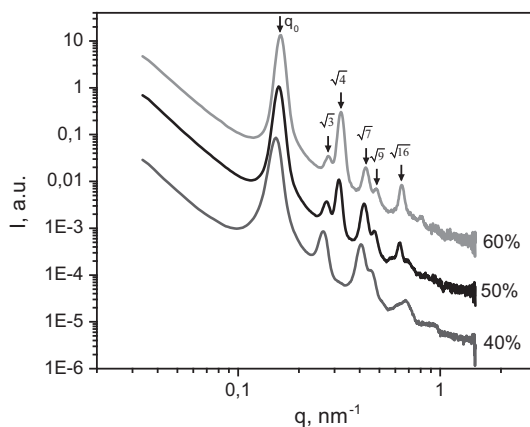


Fig. 2. SAXS spectra of blends containing 40%, 50% and 60% BCP, after complete conversion at 190 °C. Curves were vertically shifted.

$d_{\text{CYL}} = 47.1$  nm, 45.1 nm and 44.5 nm;  $d_{\text{HEX}} = 40.8$  nm, 39.0 nm and 38.5 nm. Characteristic distances decrease slightly when decreasing the volume fraction of the epoxy–amine network in the blends.

The diameter of the cylinders may be estimated from the volume fraction of PS in the blends, assuming that, at full conversion, it does not contain any residual epoxy–amine species. It is given by  $D = (32\pi f_{\text{PS}}/\sqrt{3})^{1/2}/q_0$  [38]. Resulting values for blends containing, respectively, 40, 50 and 60 wt% BCP, are:  $D = 27.1$  nm, 28.8 nm and 31.3 nm.

TEM images were used to corroborate the morphological parameters estimated from SAXS spectra. Fig. 3 shows a TEM image of the blend with 40 wt% BCP. The black domains correspond to PS, present as cylindrical cores in the HPC structure. The diameter of PS cores measured in the image is close 27 nm, in agreement with the theoretically estimated value.

Fig. 4 shows a TEM image of the blend containing 60 wt% BCP. The long cylinders are white because in the longitudinal view the black PS cores are surrounded by the PEO/epoxy matrix. The intercylinder distance estimated from the image is  $d_{\text{CYL}} = 43$  nm, in close agreement with the value calculated from the SAXS spectrum.

In order to provide an explanation for the generation of an unexpected HPC morphology in blends with the highest BCP amounts, we investigated the nanostructuring of the blend containing 60 wt% BCP after the partial cure (4 h at 135 °C attaining a conversion close to 0.12, according to Fig. 1). Fig. 5 shows a SAXS spectrum of this blend. The peak ratios  $q/q_0 = 1:2:3:4:5$  ( $q_0$  is the primary peak), indicate the presence of a lamellar morphology. The interlamellar spacing is  $d_{\text{LAM}} = 2\pi/q_0 = 30.7$  nm.

A TEM image of the partially cured blend is shown in Fig. 6. The presence of a lamellar morphology is discernible in the image, with an interlamellar distance close to the value estimated from the SAXS spectrum.

The blend containing 60 wt% BCP generated a lamellar morphology at low conversions that was transformed into the HPC morphology observed at complete conversion. This transformation should have occurred before gelation of the epoxy matrix, expected at about 60% conversion [39]. As full conversion was attained by increasing temperature from 135 °C to 190 °C, it might be argued that the L to HPC transition could have occurred by the change in the solubility of PEO produced by the temperature increase. This argument is discarded because PEO exhibits a lower-critical-solution temperature behavior in the same epoxy formulation, due to the decrease in the fraction of H-bonds by increasing temperature [31]. Therefore, a

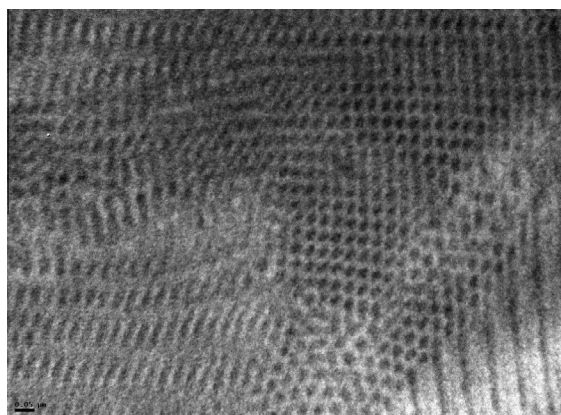


Fig. 3. TEM image of the fully cured blend containing 40 wt% BCP. The bar at the left corresponds to 50 nm.

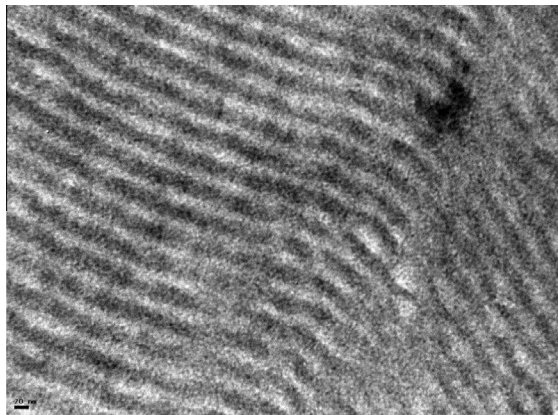


Fig. 4. TEM image of the fully cured blend containing 60 wt% BCP. The bar at the left corresponds to 20 nm.

temperature increase could only produce an order-order transition associated with a “wet” to a “dry” brush transformation (e.g., from an HPC to an L phase), that is opposite to the experimental observation.

The L to HPC transformation is depicted in Fig. 7. According to the TEM image of Fig. 6, the thickness ( $h$ ) of PS layers in the lamellar structure is about half the interlamellar distance,  $h \sim 15.4$  nm. In the HPC phase, the diameter of PS cores is 31.3 nm. Therefore, the order-order transition involves a significant coarsening of PS domains and an increase in the interdomain distance (from 30.7 nm in the L phase at 12% conversion, to 44.5 nm in the HPC phase at full conversion). It is interesting to observe that the surface per unit volume of PS lamellas ( $2/h$ ) and cylinders ( $4/D$ ) is exactly the same ( $0.13 \text{ nm}^{-1}$ ), meaning that the transition brings no penalty for the PEO chains present at the outer surface of cylindrical cores (in terms of surface insertion).

It is interesting to compare the estimated size of unperturbed PS coils with the dimensions of PS domains. The unperturbed end-to-end length of a PS coil is given by  $L_{\text{PS}} = b_{\text{PS}}N^{1/2}$ , where  $b_{\text{PS}} = 0.672$  is Kuhn's segment length of PS [30], and  $N$  is the number of segments of the PS block. This gives  $L_{\text{PS}} = 11.0$  nm. As in the lamellar thickness ( $h \sim 15.4$  nm) must contain two opposing PS coils together with an unknown fraction of epoxy-amine species, dimensions of PS coils must be significantly reduced with respect to the unperturbed coils. This means that PS coils are collapsed as expected in the presence of a poor solvent/non-solvent. When conversion increases inside the PS-rich lamella, the largest oligomers diffuse out of this phase and, at full conversion, PS domains are free of epoxy-amine species. As the epoxy-amine species diffuse out of the PS phase, PS coils can expand gaining conformational entropy. However, the expansion into lamellar domains would produce a significant reduction of the interfacial area imposing a penalty on the swelling of PEO blocks by the epoxy-amine solvent. The transformation of lamella into cylinders enables the expansion of PS coils keeping the same interfacial area. This explains the presence of an unexpected HPC morphology in blends containing a 55:45 volume ratio of both phases.

The diffusion of epoxy-amine species out PS-rich domains in the course of polymerization can also explain the increase in the intercylinder distance with conversion, reported in the literature for a BCP/epoxy blend assembled into an HPC structure [21]. This effect was corroborated for the blend with 40 wt% BCP. SAXS spectra obtained at different reaction times at 135 °C

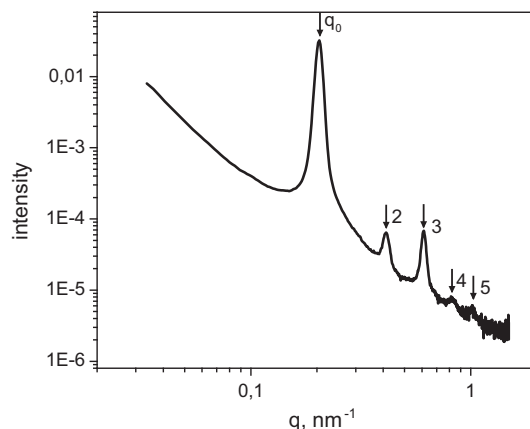


Fig. 5. SAXS spectrum of the blend containing 60 wt% BCP after the partial cure at 135 °C during 4 h.

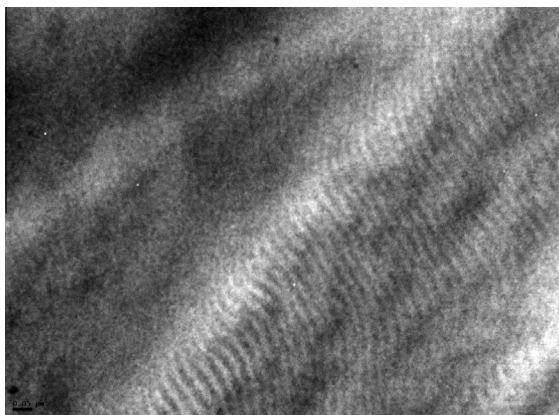


Fig. 6. TEM image of the blend containing 60 wt% BCP after the partial cure at 135 °C during 4 h. The bar at the left corresponds to 50 nm.

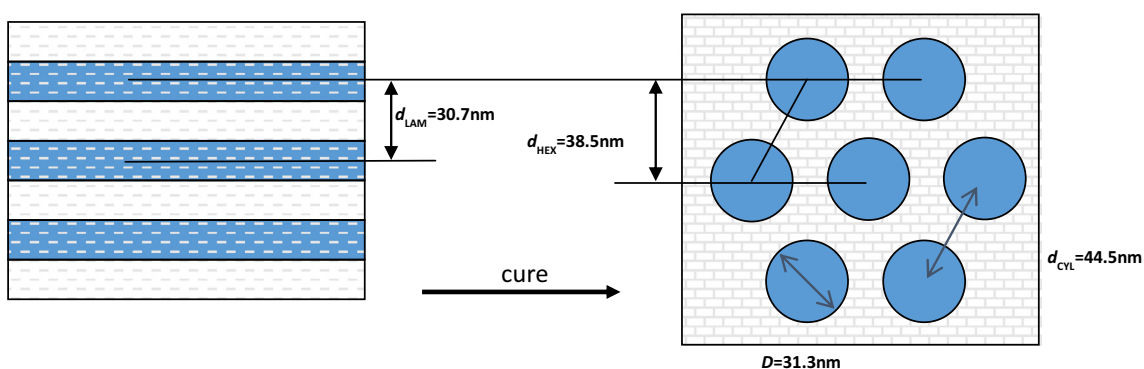


Fig. 7. Description of the L to HPC transformation.

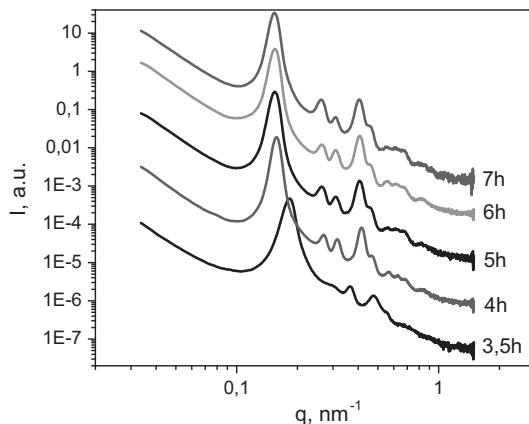


Fig. 8. SAXS spectra of a blend containing 40 wt% BCP partially cured at different periods of time at 135 °C. Curves were vertically shifted.

are shown in Fig. 8. In the spectrum taken at 3.5 h, the interdomain spacing ( $2\pi/q_0$ ) of the HPC structure was equal to 34.1 nm; it increased to 39.6 nm after 4 h reaction and stabilized at 40.8 nm in the period comprised between 5 and 7 h and after the post-cure at 190 °C.

#### 4. Conclusions

Order-order transitions in BCP/epoxy blends previously reported in the literature were explained by the partial phase separation of the *miscible* block from the epoxy solvent. These transitions go always in the sense of decreasing the interface

curvature (e.g., from HPC to L). The transition reported in this study goes in the opposite sense (from L to HPC) and was generated by the change in environment of the *immiscible* block during polymerization. This is a consequence of the partition of the reactive solvent between both phases during the initial phase separation process. The reactive solvent behaves as a poor solvent and turns into a non-solvent as polymerization progresses in the phase rich in the immiscible block. Coils of the immiscible block are collapsed in the presence of the poor solvent/non-solvent and gradually expand as the largest species of the reactive solvent diffuse to the other phase. The coil expansion can produce a change from a lamellar to a cylindrical morphology, enabling to keep the same interfacial area per unit volume. This can generate an HPC morphology outside the composition range predicted by thermodynamics. Experimental evidence of this L to HPC transition was reported in this study.

## Acknowledgements

We acknowledge the financial support of the University of Mar del Plata (Argentina), the National Research Council (CONICET, Argentina) and the National Agency for the Promotion of Science and Technology (ANPCyT, Argentina). The grant SAXS1-17067 from the Brazilian Synchrotron Light Laboratory (LNLS, Campinas, Brazil) is gratefully acknowledged.

## References

- [1] E. Girard-Reydet, J.P. Pascault, A. Bonnet, F. Court, L. Leibler, *Macromol. Symp.* 198 (2003) 309–322.
- [2] T. Fine, R. Inoubli, P. Gérard, J.P. Pascault, in: J.P. Pascault, R.J.J. Williams (Eds.), *Epoxy Polymers: New Materials and Innovations*, Wiley-VCH, Weinheim, 2010, pp. 289–302.
- [3] B. Nandan, B.K. Kuila, M. Stamm, *Eur. Polym. J.* 47 (2011) 584–599.
- [4] J. Gutierrez, I. Mondragon, A. Tercjak, *Polymer* 52 (2011) 5699–5707.
- [5] A. Tercjak, J. Gutierrez, M.D. Martin, I. Mondragon, *Eur. Polym. J.* 48 (2012) 16–25.
- [6] L. Ruiz-Pérez, G.J. Royston, J.P.A. Fairclough, A.J. Ryan, *Polymer* 49 (2008) 4475–4488.
- [7] S. Zheng, in: J.P. Pascault, R.J.J. Williams (Eds.), *Epoxy Polymers: New Materials and Innovations*, Wiley-VCH, Weinheim, 2010, pp. 81–108.
- [8] J.M. Dean, N.E. Verghese, H.Q. Pham, F.S. Bates, *Macromolecules* 36 (2003) 9267–9270.
- [9] J. Wu, Y.S. Thio, F.S. Bates, *J. Polym. Sci. Part B: Polym. Phys.* 43 (2005) 1950–1965.
- [10] Y.S. Thio, J. Wu, F.S. Bates, *Macromolecules* 39 (2006) 7187–7189.
- [11] J. Liu, Z.J. Thompson, H.J. Sue, F.S. Bates, M.A. Hillmyer, M. Dettloff, G. Jacob, N. Verghese, H. Pham, *Macromolecules* 43 (2010) 7238–7243.
- [12] C. Declet-Perez, E.M. Redline, L.F. Francis, F.S. Bates, *ACS Macro Lett.* 1 (2012) 338–342.
- [13] M.T. Bashar, U. Sundararaj, P. Mertiny, *Polym. Eng. Sci.* 54 (2014) 1047–1055.
- [14] E.M. Redline, C. Declet-Perez, F.S. Bates, L.F. Francis, *Polymer* 55 (2014) 4172–4181.
- [15] R. Francis, D.K. Baby, *Ind. Eng. Chem. Res.* 53 (2014) 17945–17951.
- [16] C. Declet-Perez, L.F. Francis, F.S. Bates, *Macromolecules* 48 (2015) 3672–3684.
- [17] M. Naguib, M. Sangermano, L.C. Capozzi, D. Pospiech, K. Sahre, D. Jehnichen, H. Scheibner, B. Voit, *Prog. Org. Coat.* 85 (2015) 178–188.
- [18] R. Matadi Boumbimba, C. Froustey, P. Viot, P. Gerard, *Compos. Part B Eng.* 76 (2015) 332–342.
- [19] Z. Heng, Y. Chen, H. Zou, M. Liang, *RSC Adv.* 5 (2015) 42362–42368.
- [20] M.A. Hillmyer, P.M. Lipic, D.A. Hajduk, K. Almdal, F.S. Bates, *J. Am. Chem. Soc.* 119 (1997) 2749–2750.
- [21] P.M. Lipic, F.S. Bates, M.A. Hillmyer, *J. Am. Chem. Soc.* 120 (1998) 8963–8970.
- [22] F. Meng, S. Zheng, W. Zhang, H. Li, Q. Liang, *Macromolecules* 39 (2006) 711–719.
- [23] F. Meng, S. Zheng, H. Li, Q. Liang, T. Liu, *Macromolecules* 39 (2006) 5072–5080.
- [24] H.E. Romeo, I.A. Zucchi, M. Rico, C.E. Hoppe, R.J.J. Williams, *Macromolecules* 46 (2013) 4854–4861.
- [25] C.C. Riccardi, J. Borrajo, R.J.J. Williams, *Polymer* 35 (1994) 5541–5550.
- [26] R.J.J. Williams, B.A. Rozenberg, J.P. Pascault, *Adv. Polym. Sci.* 128 (1997) 95–156.
- [27] M. Rico, J. López, B. Montero, C. Ramírez, R. Bouza, *Eur. Polym. J.* 47 (2011) 2432–2441.
- [28] M. Rico, J. López, B. Montero, R. Bellas, *Eur. Polym. J.* 48 (2012) 1660–1673.
- [29] M. Rico, J. López, B. Montero, R. Bouza, F.J. Diez, *Eur. Polym. J.* 58 (2014) 125–134.
- [30] S.H. Choi, F.S. Bates, T.P. Lodge, *Macromolecules* 47 (2014) 7978–7986.
- [31] A.B. Leonardi, I.A. Zucchi, R.J.J. Williams, *Eur. Polym. J.* 65 (2015) 202–208.
- [32] M. Gervais, B. Gallot, *Makromol. Chem.* 174 (1973) 193–214.
- [33] J. Ruokolainen, G. Ten Brinke, O. Ikkala, M. Torkkeli, R. Serimaa, *Macromolecules* 29 (1996) 3409–3415.
- [34] M.W. Matsen, *Macromolecules* 45 (2012) 2161–2165.
- [35] D.A. Hajduk, S.M. Gruner, P. Rangarajan, R.A. Register, L.J. Fetters, C. Honeker, R.J. Albalak, E.L. Thomas, *Macromolecules* 27 (1994) 490–501.
- [36] T. Hashimoto, T. Kawamura, M. Harada, H. Tanaka, *Macromolecules* 27 (1994) 3063–3072.
- [37] V.F. Scalfani, E.F. Wiesenauer, J.R. Ekbald, J.P. Edwards, D.L. Gin, T.S. Bailey, *Macromolecules* 45 (2012) 4262–4276.
- [38] S. Sakurai, T. Momii, K. Taie, M. Shibayama, S. Nomura, T. Hashimoto, *Macromolecules* 26 (1993) 485–491.
- [39] J.P. Pascault, H. Sautereau, J. Verdu, R.J.J. Williams, *Thermosetting Polymers*, Dekker, New York, 2002. p. 89.